International Journal of Engineering Research & Technology (IJERT)
ISSN: 2278-0181
Vol. 15 Issue 06 , June - 2026

Prediction of Temperature Distribution Through Transient Thermal Analysis for the Weld Joints of Austenitic Stainless-Steel Plates and Tubes Used for Nuclear Applications

S Dineshkumar
(Corresponding *Author*)
PG Student, Department of Mechanical Engineering
PRIST deemed to be University
Thanjavur -613 403, Tamil Nadu, India

M Sudhahar (Co-*Author*)
Asst Prof, Department of Mechanical Engineering
PRIST deemed to be University
Thanjavur -613 403, Tamil Nadu, India

R Baskaran (Co-*Author*)
Asst Prof, Department of Mechanical Engineering
PRIST deemed to be University
Thanjavur -613 403, Tamil Nadu, India

Abstract - Welding simulation is a complex process involving more procedures and methodologies and requiring numerous input variables to accurately represent the welding conditions and find the reliable real-time outputs. This paper is built on the finite elements method, to predict the temperature distribution of austenitic stainless steel plates and tubes weld joint of multi-pass GTAW welding simulation.

Transient thermal analysis of the weld process is carried out to model by moving heat source and birth and death element method to find temperature distribution in the heat-affected zone (HAZ) using the finite element software ANSYS APDL methods. The model and developed procedure effectively incorporates temperature-dependent material properties at various temperatures till melting range of steel; and using calculated various inputs welding parameters, weld metal solidification, and convective & radiative heat transfer boundary conditions.

The numerical model was developed to reproduce the experimental observations by S Murugan, and using the mentioned method, the predicted results were compared with experimental data to validate the simulation approach.

The same approach of sequential multiple welding passes in the weld joint is simulated in APDL, which effectively replicates welding by moving heat input model in tube-to-tube weld joint. The obtained temperature distribution will be used as input for structural analysis for residual stress estimation and structural integrity assessment of the welded joints of Advanced Heat Exchanger tubes.

Keywords ANSYS APDL, Welding Simulation, temperature distribution, transient thermal analysis, moving heat source, residual stresses, finite element method, heat exchanger tubes

1.0 INTRODUCTION

Welding is an essential manufacturing process technique widely used for joining similar or dissimilar materials through fusion. It is a backbone of modern industrial production due to its high efficiency, reliability, and capability to join a broad range of engineering materials. The performance and integrity of welded structures are strongly governed by the thermal conditions generated during the welding operation.

The welding process comprise a continuously moving heat source that introduces localized heating and produces sharp temperature gradients within the material. These gradients result in convoluted thermal cycles during heating and cooling, which significantly transforms the microstructure and mechanical properties of the weldment. The resulting non-uniform temperature zone leads to thermal strains and uneven plastic deformation, ultimately leads to increase residual stresses and distortions in welded joints. The effect of residual stresses may be beneficial or detrimental, depending on their magnitude, sign and distribution with respect to load induced stress. In most of the cases residual stresses are tensile in nature and have detrimental effect on the fatigue strength of the components. If the service stresses were superimposed with the residual stresses which already present in the welded regions, it may enhance the failure of the material. In worst cases, the residual stress may be equal to the tensile yield strength of the material.

In nuclear industries, which warrant high level of reliability in performance of safety related components, failure of components can have severe safety and financial consequences. In these components one of the critical locations is weld joints which have considerable

International Journal of Engineering Research & Technology (IJERT)
ISSN: 2278-0181
Vol. 15 Issue 06 , June - 2026

residual stress apart from the normal operating loads. Therefore, reliable prediction and effective control of residual stresses in welded connections play a vital role in preserving long-term structural stability and operational safety for nuclear components.

The challenges and high costs involved in experimentally measuring welding thermal fields and residual stresses have led to the widespread adoption of numerical simulation techniques for their evaluation. ANSYS Parametric Design Language (APDL) serves as an effective tool for welding analysis by integrating moving heat source formulations, temperature-dependent material characteristics, and transient thermal simulation techniques. In this work, a three-dimensional transient thermal simulation analysis of weld joint is carried out for analysing the residual stresses in the typical weldments of Heat Exchanger tubes. The analysis of welded structures is performed using finite element code ANSYS and has validated against the experimental works done by Murugan et.al. [3]

1.1 objective and scope

The objective of transient thermal analysis is to estimate the temperature distribution in the heat affected zone of weld joint. The temperature distribution is estimated using temperature dependent material properties as well as convective and radiative mode of heat transfer in the joints. The analysis procedure is validated with experimental results and same is used for the temperature distribution in the weld joints in heat exchanger tubes. The temperature distribution will be used as input for residual stress estimation in structural analysis.

1.2 Summary of The Research

The validation of procedure deals with the modelling of weld geometries in ANSYS, use of temperature dependant material properties, expressions for applying weld heat source as a heat generation, account of the radiation mode of heat transfer effects in convective heat transfer coefficient, getting the temperature distribution profiles and validating the results with experimental values [3]. Thermal analysis of heat exchanger tubes deals with the modelling of tubes, weld specifications and temperature distribution in weldments.

2.0 METHODS AND MATERIALS

2.1. Validation of Procedure

Transient thermal analysis of weld is validated against the experimental works done by S.Murugan et al [3], before proceeding with the thermal analysis of welds of Heat Exchanger tubes. The steps involved in the transient thermal analysis are explained in details in following sections:

2.2. Weld Geometry

The dimensions of the plate used in experiment [3] were 70x50x6mm. Butt welding was carried out on the plates as shown in figure. The root gap allowed for welding is 2.5mm. 'V' groove of 60° has provided in the plate for welding. The position of thermocouples used in experiment was shown in the figure 2.1.

The weld joints in Advanced Heat Exchanger tubes are 'V' groove butt joints. So Weld joint of the plate for validation also modelled as a 'V' groove butt joint in theoretical analysis. Since the experimental results are not available for the 'V' groove butt joint welds, the theoretical results are compared with the bead-on-plate welding process with the same heat inputs [3]. To simulate the actual welding conditions, heat input for welding is applied as heat generation on elements.

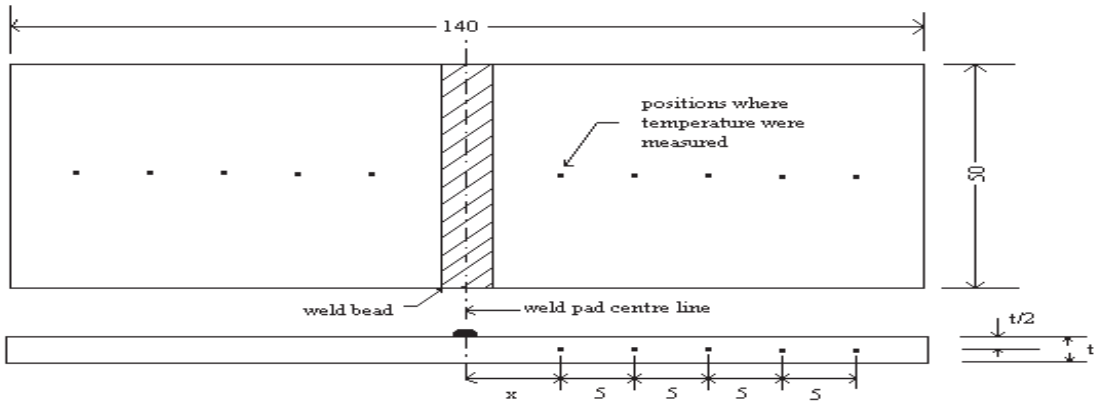

Fig. 2.1: Schematic diagram of weld plate used in experiments, 't' is plate thickness of 6mm and x is 9mm

International Journal of Engineering Research & Technology (IJERT)
ISSN: 2278-0181
Vol. 15 Issue 06 , June - 2026

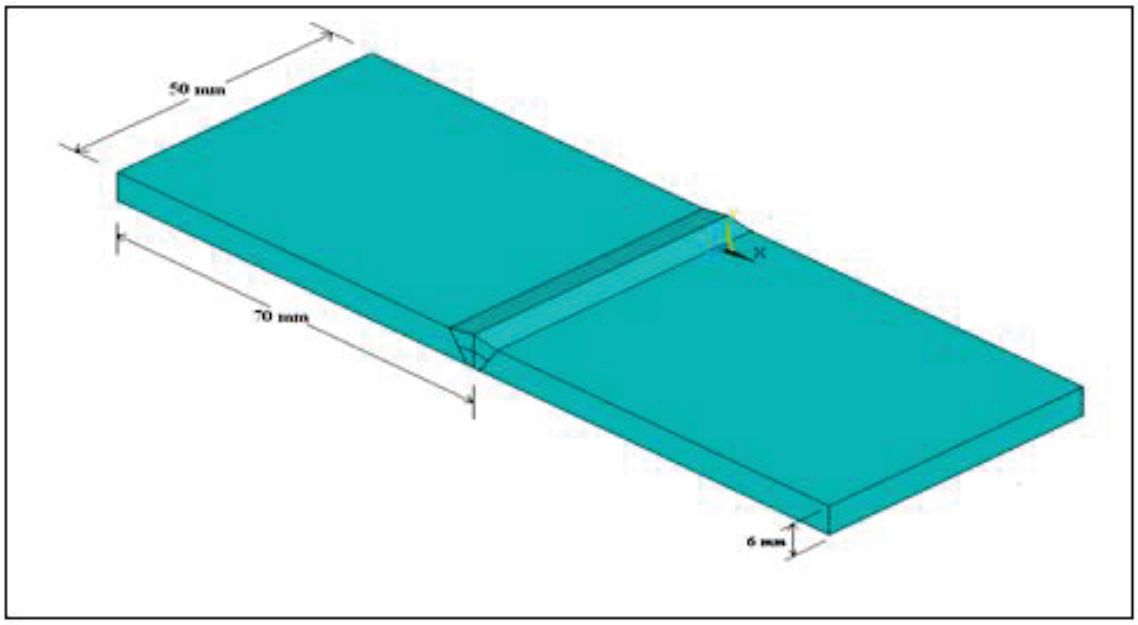

Fig. 2.2: Solid model of the weld plate used in the experiment

2.3. Material Properties

Stainless steel plates, AISI type 304L has taken for our analysis. The temperature dependent material properties of SS304L [2, 3, 9, 10] are given below.

Table 2.1: Temperature dependent material properties of the stainless steel 304L

Temperature (ºC)	Thermal conductivity (W/m(ºC)	Specific heat (J/KgºC)	Density (Kg/m^3)	Enthalpy (J/Kg)
100	14.12	325.0	8000	3.62E+08
500	20.60	367.5	8000	1.83E+09
900	27.20	410.2	8000	3.30E+09
1300	33.77	452.8	8000	4.77E+09
1355	34.42	458.0	8000	5.01E+09
1365	34.73	459.7	8000	5.07E+09
1368	34.75	460.1	8000	5.13E+09
1370	34.77	550.0	8000	5.18E+09
1372	34.80	760.0	8000	5.22E+09
1374	37.03	2500.0	8000	5.27E+09
1376	39.26	2766.4	7591	5.31E+09
1378	41.50	2770.8	7579	5.35E+09
1380	43.72	2775.9	7565	5.40E+09
1387	51.53	2794.0	7516	5.54E+09
1467	142.70	2902.6	7235	6.87E+09
1474	146.60	2913.8	7207	6.92E+09
1478	151.20	2700.0	7200	6.94E+09
1480	153.80	2300.0	7200	6.95E+09
1482	156.40	1000.0	7200	6.96E+09
1487	161.00	660.0	7200	6.98E+09
1493	161.00	620.0	7200	7.00E+09
1500	161.00	599.8	7200	7.00E+09
1530	161.00	596.4	7200	7.00E+09
1800	161.00	566.4	7200	7.00E+09

The variation of material properties with temperature has shown in the figures 2.3, 2.4, 2.5.

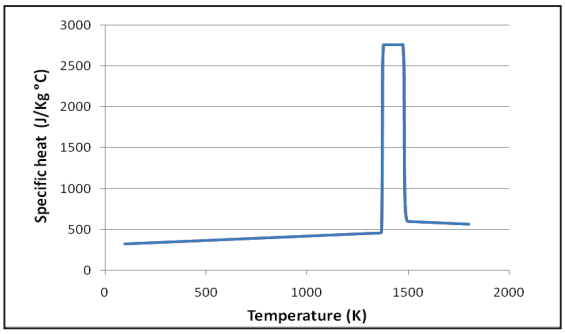

Fig. 2.3: Variation of specific heat with temperature

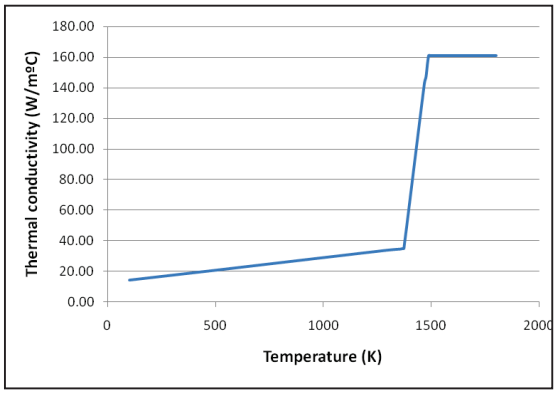

Fig. 2.4: Variation of thermal conductivity with temperature

International Journal of Engineering Research & Technology (IJERT)
ISSN: 2278-0181
Vol. 15 Issue 06 , June - 2026

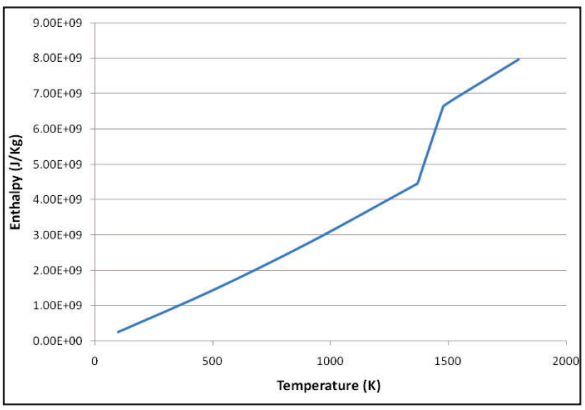

Fig. 2.5: Variation of enthalpy with temperature

To compensate for weld pool convective heat transfer, an artificially high conductivity value for the metal was used in the weld pool. The thermal conductivity value was increased to 160 W/m ^{o}C in the weld pool [3]. The thermal conductivity verses temperature graph shows the steep rise at the weld pool. The release or absorption of latent heat of fusion can be simulated by an artificial increase in the value of specific heat over the melting range. The melting range is 1375 – 1475 ^{o}C [3]. The latent heat at the melting range was taken as $2.1x10^{9}$ J/m^{3}. Latent heat of fusion is the reason for the sudden rise of the specific heat verses temperature curve during the melting range. The density of the material at the solid state is 8000 Kg/m^{3}. The density of the material at the liquid state is 7200Kg/m^{3}. Enthalpy value rise with temperature also shown in the figure above. It always increases with temperature.

2.4. Finite Element Model

The finite element tool, ANSYS has used for the analysis. 'Plane55' element is selected for two dimensional thermal analysis and 'Solid70' element is selected for three dimensional thermal analysis, whereas 'Solid70' element has eight nodes with a single degree of freedom, temperature at each node. This element can be used for 3-D steady-state or transient thermal analysis. This element should be replaced by an equivalent structural element for structural analysis [2].

Brick element is selected for mapped meshing. The weld volumes are meshed with fine mesh. The other volumes are meshed with coarse mesh. For the transient thermal analysis with moving heat source, the spatial stability conditions are checked for mesh refinement. Since the model taken for analysis is symmetric with 'y-z' plane. The advantages of symmetric boundary conditions also utilized in this analysis.

The finite element meshed portion of the welded region is shown in figure 2.7. The welding has done in two passes. Initially both the volumes are created and deactivated. The same is activated during welding operation by element birth and death features of ANSYS.

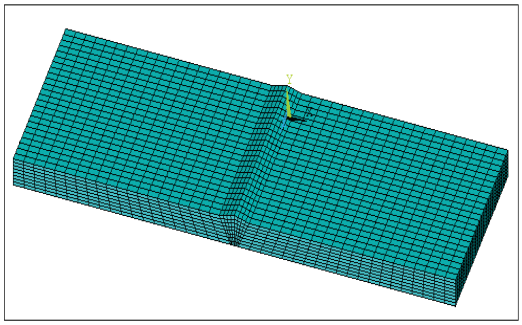

Fig. 2.6: Isometric view of welded component meshed with 3-D element

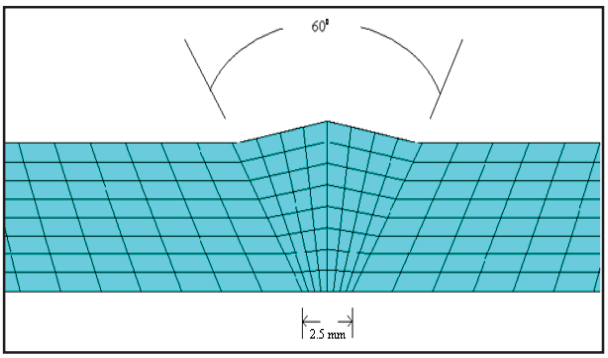

Fig. 2.7: Finite element model of the weld area

2.5. Boundary Conditions

Heat input is given as a heat generation in the welding region including the effects of moving heat source. For the first pass of welding operation, the elements in the weld volume are selected and the heat generation is applied for the specified time interval according to the weld arc speed. The heat generation value has been calculated as given below [1].

Heat input =

$$\eta \times \frac{V.A}{\upsilon}$$

Where,

'V' is the weld arc voltage, 'A' is the weld arc current

'η' is the weld arc efficiency, 'υ' is the arc travel speed

For first pass of welding,

Weld voltage (V) is 22V, weld current (A) is 60 - 65A, weld speed (υ) is 2.00 mm/s and

International Journal of Engineering Research & Technology (IJERT)
ISSN: 2278-0181
Vol. 15 Issue 06 , June - 2026

The arc efficiency of the manual metal arc welding process is reported to be 70% to 85% [1], some investigators has used a value of 75%. So in the present analysis the arc efficiency has taken as 75%

Average heat input = 515.625 J/mm

= 1031.25 $J/\sec$

Heat generation rate = heat input / weld volume

= heat input / (weld area × weld element length)

= heat input / (weld area × width/ number of divisions)

= 1.46×10^8 ×number of divisions/ width $J/m^3 \sec$

For second pass of welding,

Weld voltage (V) is 21V, weld current (A) is 130 - 140A, weld speed (υ) is 2.03 mm/s and

Weld arc efficiency (η) is 75 % [11].

Average heat input = 1047.41 J/mm

= 2126.25 $J/\sec$

Heat generation rate = heat input / weld volume

= heat input / (weld area × weld element length)

= heat input / (weld area × width/ number of divisions)

= 1.825×10^8 ×number of divisions/ width $J/m^3 \sec$

Weld arc efficiency (η) is 75 % [11].

Effect of radiation becomes at high temperatures, where it dominates over the surface convection and appears primary mechanism of heat loss from the surface. During welding operation high heat is applied to the weld beads. So radiation mode of heat transfer will happen. Further, to capture the effect of convective and radiative heat loss from the surface, temperature dependant equivalent heat transfer coefficient comprising of convection and radiation is calculated by using the equation below. The value of emissivity (ε) used in the analysis is 0.40 [3].

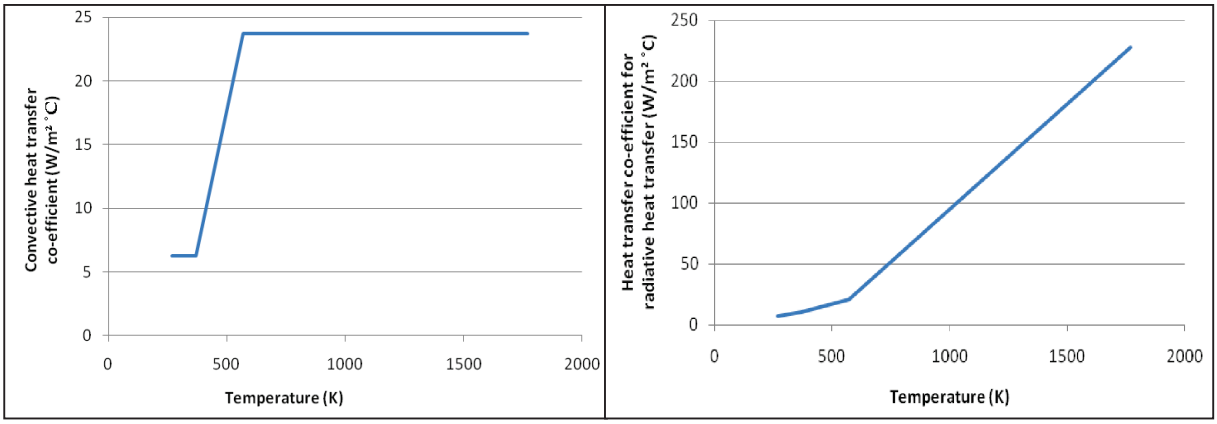

Fig. 2.8: Variation of heat transfer co-efficient with temperature for convection and radiation mode of heat transfer

$$h_{tot} = \frac{\varepsilon.\sigma.((T+273)^4 - (T_\alpha + 273)^4}{(T - T_\alpha)} + h_{conv}$$

Where, σ is the Stefan- Boltzmann constant (5.699×10^{-8} $W/m^2.k^4$). Temperature dependant convection heat transfer co-efficient [9] used in the analysis are given in the figure 2.8.

Time for transient analysis has calculated by the weld arc speed. The time given for the movement of heat is the ratio of weld element length to the arc velocity. First, the heat generation is applied on the first elemental volume for the above specified time interval and then the heat generation is removed and the same is applied on the next element and so on. After doing the whole first pass weld, the plate is allowed for some time to cool. Then the second weld pass is carried out by the same way.

International Journal of Engineering Research & Technology (IJERT)
ISSN: 2278-0181
Vol. 15 Issue 06 , June - 2026

2.6. Mesh stabilization Study

Before analysing the results, convergence study was carried out for the same material with same dimensions. By varying the element size in mesh, the results are compared. Particularly by varying the number of divisions of the whole weld volume in the longitudinal direction of weld, the convergence study was carried out. The variation of maximum temperature, thermal gradient and thermal heat flux at the beginning of the second pass were analysed. The results are shown in figure 2.9.

2.7. Temperature Distribution

The temperature profiles have drawn at different points in the heat affected zone.

As convenient for comparison the same points at which the experiment was carried out in Murugan et al [3] has chosen for analysis.

The distance of the points from the weld centre line are 9mm, 14mm, 19mm and 24mm respectively.

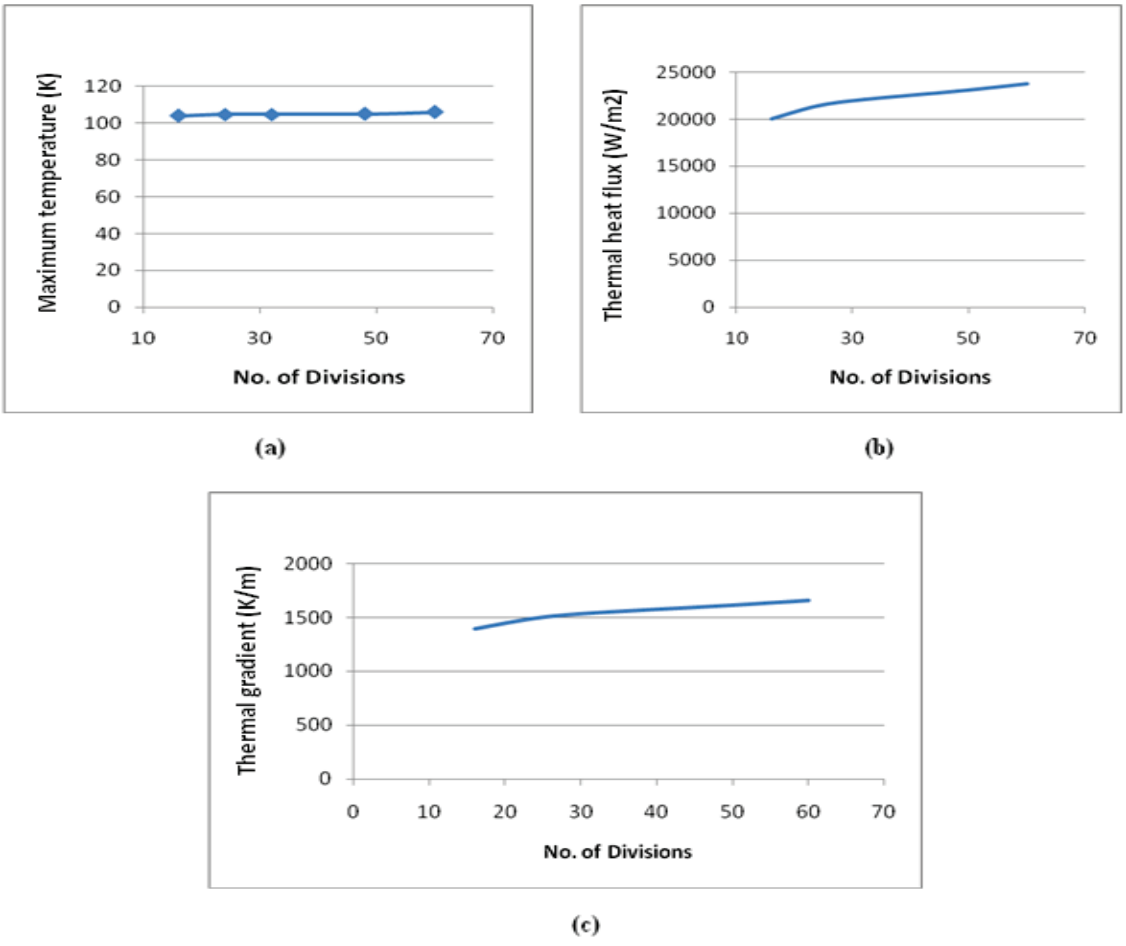

Fig. 2.9: Variation of (a) maximum temperature, (b) thermal gradient and (c) thermal heat flux with varying mesh size

The figure has drawn for the change in values with number of divisions in longitudinal direction of weld. The variation of the maximum temperature, maximum thermal gradient and maximum thermal heat flux were analysed for convergence study. Since the variations are very small (within 5%), the element length with 1.5625mm in longitudinal direction of weld (number of divisions 32 in longitudinal direction of weld) is selected for further analysis

The temperature distribution at various points in the weld bead also analysed and it is shown in figure 2.10. The temperature distributions of various points along the weld bead during the first pass of welding, temperature plot of the plate at the end of first pass of weld and temperature distribution at various points in the heat affected zone are shown in figures 2.13 & 2.14.

International Journal of Engineering Research & Technology (IJERT)
ISSN: 2278-0181
Vol. 15 Issue 06 , June - 2026

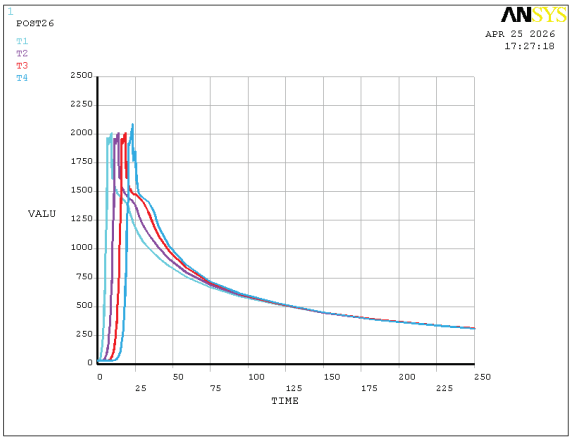

Fig. 2.10: Temperature distribution at various points in the weld bead

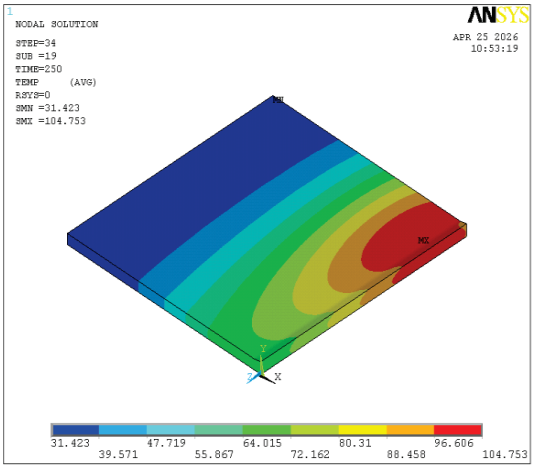

Fig. 2.11: Temperature plot of the plate at the end of first pass of weld

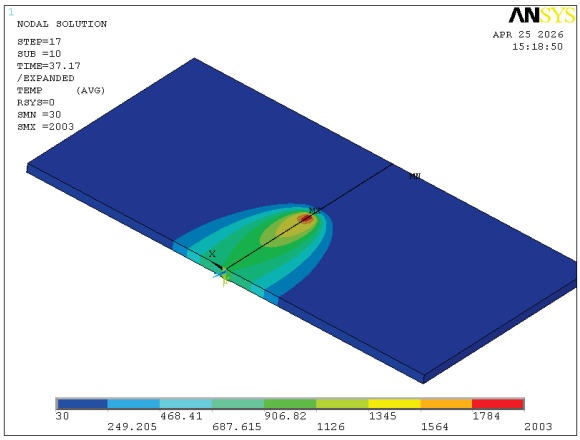

Fig. 2.12: A schematic view of the component at the half welded position

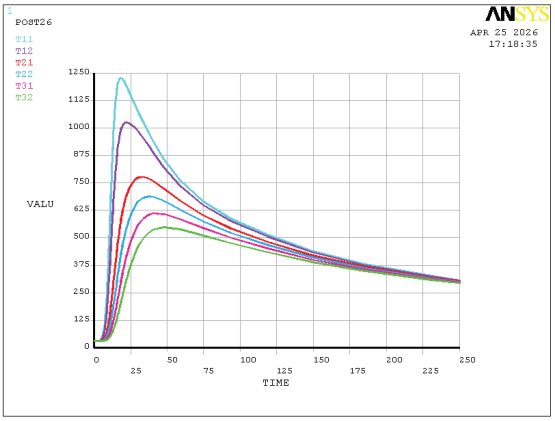

Fig. 2.13: Temperature distribution at various points in the heat affected zone before the second pass begins

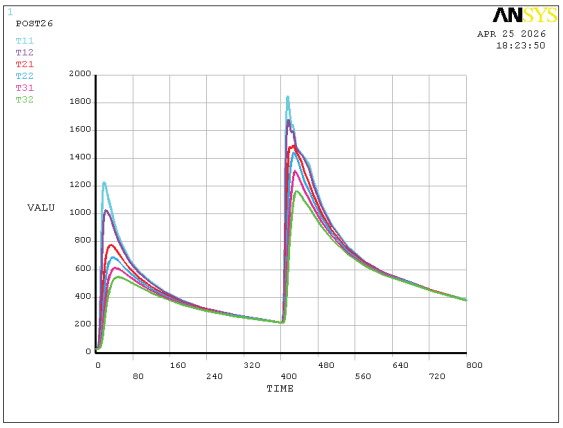

Fig. 2.14: Temperature distribution at various points in the heat affected zone after the welding is over

2.8. Comparison of Results

The theoretically obtained values of temperature against the experimentally measured values of temperature in the heat affected zone are compared. The comparisons of the values are shown in figure 2.15.

Here the maximum temperature and the temperature at various time steps calculated by theoretical analysis has compared with experimental values [3].

The maximum temperature calculated from theoretical analysis at the distance of 9mm from the weld centreline in the heat affected zone varies 3.6% from experimental value.

International Journal of Engineering Research & Technology (IJERT)
ISSN: 2278-0181
Vol. 15 Issue 06 , June - 2026

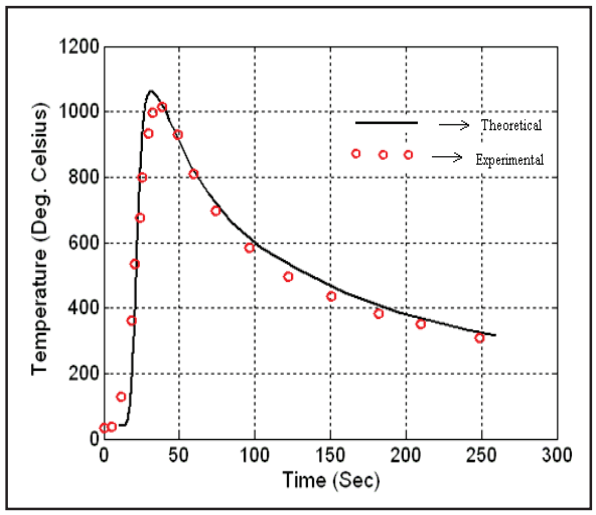

Fig. 2.15: Comparison of experimental and theoretical values of maximum temperature at the distance of 9mm from the weld centreline .

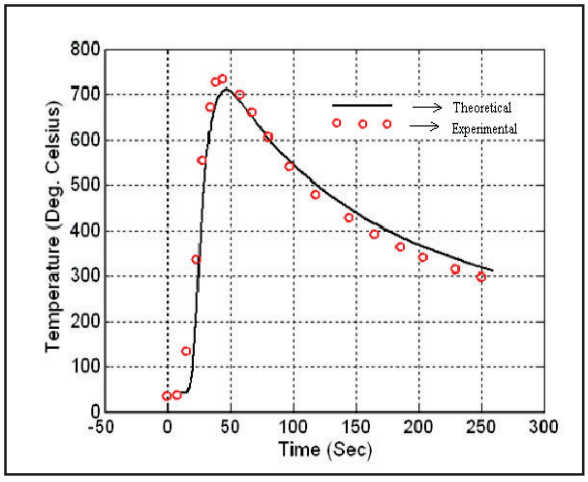

Fig. 2.16: Comparison of experimental and theoretical values of maximum temperature at the distance of 14mm from the weld centreline

Temperature at various time steps at the distance of 9mm from the weld centreline varies less than 4% at all time steps in the heat affected zone from experimental value. Similarly the theoretically obtained values at the distance of 14mm and 19mm from the weld centreline in the heat affected zone has compared with the experimentally calculated values. The theoretically obtained results are closely matching with the experimental results. The values vary less than 4% at all time steps in the heat affected zone. The results are shown in the figures 2.16 & 2.17.

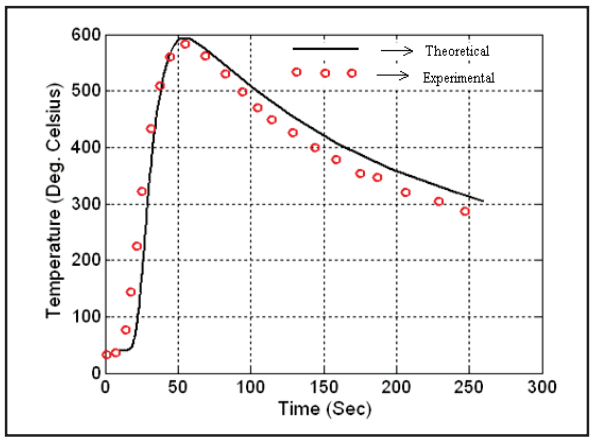

Fig. 2.17: Comparison of experimental and theoretical values of maximum temperature at the distance of 19mm from the weld centreline

Thus, it is observed that the theoretical values obtained from developed procedure are closely matching with the experimental values. Therefore same is used for the thermal transient analysis of heat exchanger Tubes.

3.0 Thermal Analysis of Advanced Heat Exchanger Tubes

These tubes are welded with inner and outer heaters of advanced heat exchanger by tube to tube joints. Gas Tungsten Arc Welding (GTAW) is used for making the weld joints. A thermal analysis has carried out on the welded joints to account the residual stresses in weldments of advanced heat exchanger tubes. The weld

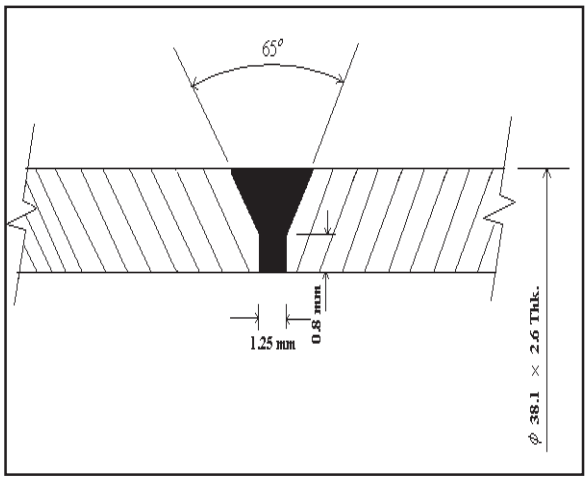

Fig. 3.1: Schematic diagram showing the details of welded joints of Advanced Heat Exchanger tube

International Journal of Engineering Research & Technology (IJERT)
ISSN: 2278-0181
Vol. 15 Issue 06 , June - 2026

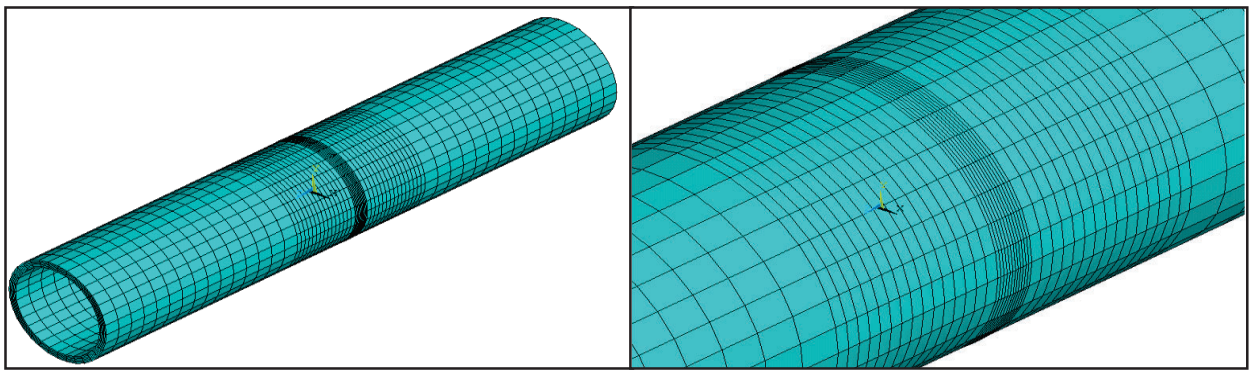

Fig. 3.3: Expanded view of finite element model of the weld area

geometry of advanced heat exchanger tubes has shown in the figure 3.1.

3.1. Modelling of Tubes

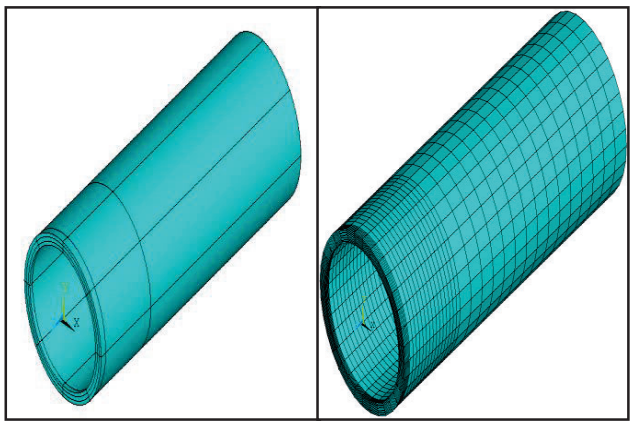

Fig. 3.2 Schematic diagrams shows the finite element modals of Advanced Heat Exchanger tubes

The outer diameter of the advanced heat exchanger tube is 38.1 mm and the thickness of the tube is 2.6mm. Tubes were modelled by 'Solid70' element ANSYS. Since the welding is carried out on the tubes by three passes, three volumes are created at the welded region.

The features of symmetry was utilised in the analysis. The weld regions and the heat affected zone were meshed with

fine mesh. The temperature dependant material properties has used for the analysis.

3.2. Weld Specifications

The weld joint design is single 'V' groove butt joint. The weld is taking place by three passes. One root pass followed by the two subsequent passes. Direct current with straight polarity has been used for all passes of welding. The details of the weld specifications are given in the table below.

Table 3.1: Weld parameters

Heat input for welding has been calculated as per the expressions given in validation procedure of thermal analysis. Then the heat input has applied as a heat generation in the welded regions. The temperature dependant convective and radiative heat transfer co-efficient boundary conditions were applied as per the validation procedure. The heat generation has applied on the elements in the welded region for a time period according to the arc travel speed.

3.3. Temperature Distribution

The temperature distribution at the end each pass of welding has given in the figure. Also the Temperature distribution profiles at weld bead have given in the figures 3.4, 3.5 and 3.6.

Weld pass number	Welding process	Filler metal diameter (mm)	Current type and polarity	Amp range (A)	Voltage range (volts)	Travel speed range (mm/min)
1	GTAW	1.2	DCEN Straight	40-48	11-13	40-50
2	GTAW	1.6	DCEN Straight	60-75	11-14	60-70
3	GTAW	1.6	DCEN Straight	70-80	11-14	60-70

International Journal of Engineering Research & Technology (IJERT)
ISSN: 2278-0181
Vol. 15 Issue 06 , June - 2026

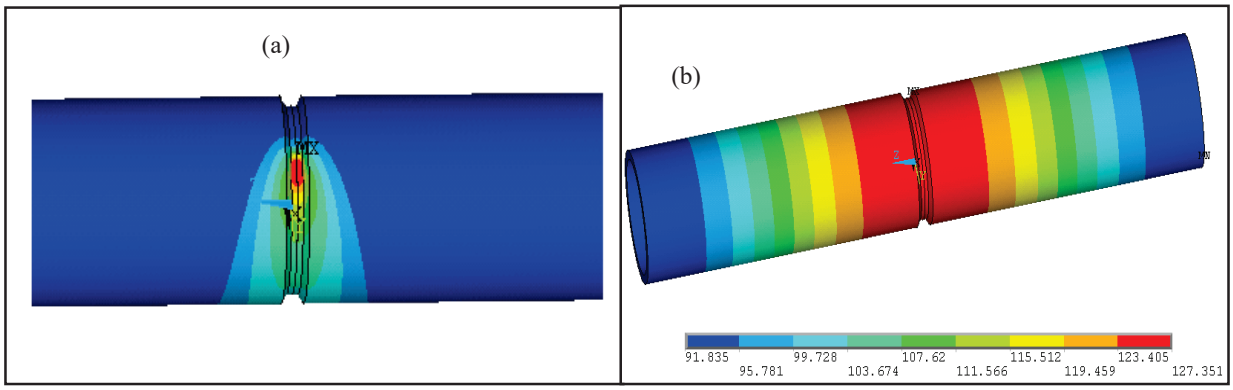

Fig. 3.4: Temperature distribution in the weld joints during root pass of welding (a) during welding (b) after 400 Seconds of cooling

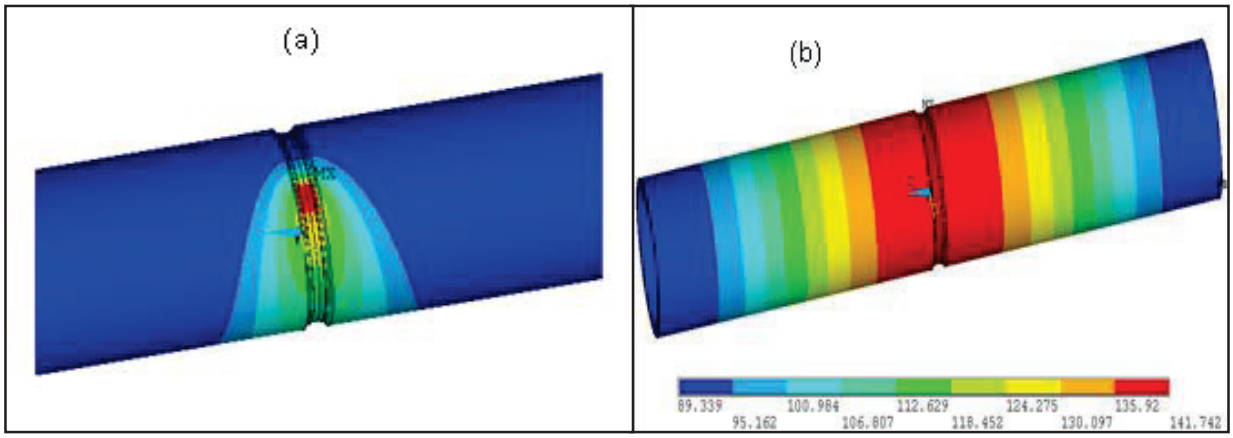

Fig. 3.5: Temperature distribution in the weld joints during second pass of welding (a) during welding (b) after 400 Seconds of cooling

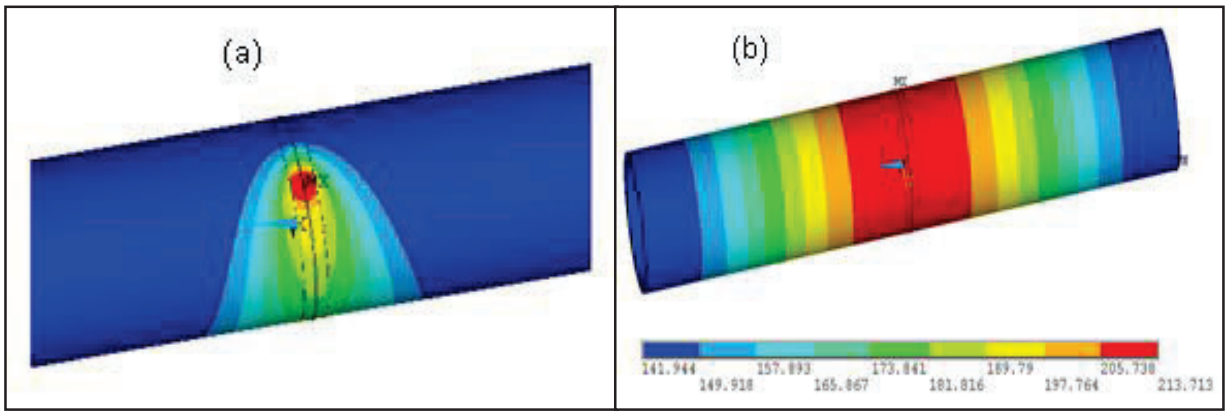

Fig. 3.6: Temperature distribution in the weld joints during final (third) pass of welding (a) during welding (b) after 400 Seconds of cooling

International Journal of Engineering Research & Technology (IJERT)
ISSN: 2278-0181
Vol. 15 Issue 06 , June - 2026

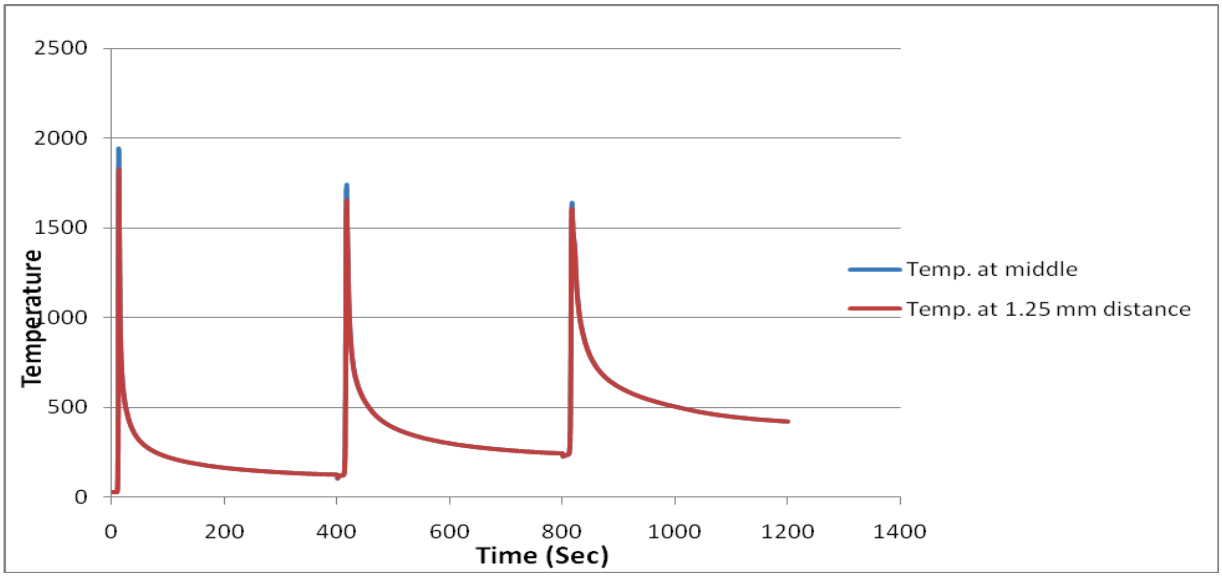

Fig. 3.7: Temperature distribution profiles of the tube at the weld bead and 1.25 mm distance from the middle point of weld

The temperature distributions obtained from thermal analysis can be used as the input for residual stress evaluation in structural analysis.

4.0 RESULTS AND DISCUSSION

The transient thermal analysis of the SS304L welded joint was carried out using ANSYS APDL to predict the temperature evolution during the welding process. A moving heat source was applied along the weld path to simulate actual welding conditions. The primary objective of the simulation was to obtain the transient temperature field, evaluate thermal gradients, and validate the numerical results with available experimental data.

4.1 Temperature Distribution in Weld Zone

The results of the thermal simulation indicate that a highly localized temperature field is developed around the welding heat source. The maximum temperature is observed directly at the weld centerline where the heat flux is applied.

In SS304L stainless steel, the recorded thermal profile reveals that peak temperatures surpass the material's melting range (approximately 1400–1500°C), thereby confirming full metallurgical fusion within the weld zone. As the arc heat source traverses the joint, the zone of maximum thermal intensity migrates in tandem, underscoring the inherently transient and dynamic character of the welding thermal cycle. A pronounced thermal gradient develops perpendicular to the weld centerline, with temperatures attenuating sharply from the fusion boundary into the adjacent base metal — a behavior largely governed by the thermal conductivity of the material.

This spatially non-uniform temperature distribution manifests as extreme localized heating in the immediate weld vicinity, while regions further from the fusion zone experience comparatively modest temperature rises. This concentrated thermal input is an intrinsic feature of arc-based welding and exerts a decisive influence on three critical outcomes: the lateral extent of the heat-affected zone (HAZ), the magnitude and distribution of residual stresses, and the progression of microstructural transformations in SS304L. The successive thermal excursions of rapid heating followed by accelerated cooling drive grain coarsening, alter austenitic phase stability, and ultimately dictate the mechanical performance of the completed weld joint.

4.2 Thermal Gradient and Heat-Affected Zone (HAZ)

Simulation results reveal a pronounced attenuation of temperature with increasing lateral distance from the weld centerline. Within an approximate temperature band of 600°C to 900°C, the heat-affected zone (HAZ) is distinctly demarcated — a region where the base metal, though not raised to fusion temperatures, is subjected to significant thermal excursions capable of modifying both grain morphology and mechanical response. The spatial extent of the HAZ is observed to be strongly governed by two interacting parameters: the net heat input delivered during welding and the thermal conductivity characteristics of SS304L. Given the inherently low thermal conductivity of austenitic stainless steels, heat dissipation into the surrounding material is comparatively sluggish, producing a HAZ that is geometrically narrower

International Journal of Engineering Research & Technology (IJERT)
ISSN: 2278-0181
Vol. 15 Issue 06 , June - 2026

yet thermally more severe relative to that observed in carbon steel weldments.

Under idealized welding conditions — uniform energy input and constant travel speed — the computed thermal field displays bilateral symmetry about the weld centerline, reflecting balanced heat flow on either side of the joint. In practical welding scenarios, however, departures from this symmetrical distribution are not uncommon and may serve as precursors to geometric distortion or the buildup of asymmetric residual stress fields within the weldment.

4.3 Thermal Cycles and Cooling Behavior

Temperature–time histories were extracted at selected nodal locations positioned at 9 mm, 14 mm, and 19 mm from the weld centerline. The results show a rapid increase in temperature as the heat source approaches the measurement point, followed by a peak temperature when the heat source is directly aligned, and then a gradual cooling phase once the heat source moves away.

The cooling rate is observed to be higher immediately after the peak temperature is reached. This rapid cooling is transfer by conduction into the nearby colder material. That the consecutive a typical welding heating-cooling pattern of thermal cycle, determining residual stress formation and metallurgical transformations.

The weld centreline closer nodes expose peak temperature and faster cooling rates compare to away. This variation highlights the non-uniform thermal response of the welded joint.

4.4 Validation with Experimental Results

The numerical results obtained from ANSYS APDL were validated against experimental temperature measurements reported for similar SS304L welding conditions. A good agreement between numerical and experimental results is observed.

At a distance of 9 mm from the weld centerline in the heat-affected zone, the maximum temperature deviation between simulation and experiment is approximately **3.6%**. Similarly, temperature values at different time steps for locations at 9 mm, 14 mm, and 19 mm show deviations within **4%**, indicating strong correlation.

This close agreement confirms that the developed finite element model and moving heat source formulation are capable of accurately predicting transient thermal behavior during welding. The validation also confirms that appropriate material properties, boundary conditions, and heat input parameters have been used in the simulation.

4.5 Thermal Behavior in Tube Welding Application

The validated thermal model was further extended to analyze heat exchanger tube welding applications. The same transient thermal approach was applied to cylindrical geometry to study temperature distribution in tube-to-tube welding conditions.

The results indicate that heat concentration is more localized in tube geometries due to curvature effects and reduced heat dissipation area. The temperature gradients are steeper compared to flat plate welding, which may lead to higher residual stresses in tube welds.

The modeling approach demonstrates that the developed ANSYS APDL simulation can be effectively used for complex geometries such as tubes, cladding surfaces, and multi-pass welds.

4.6 Heat Transfer Mechanism and Model Reliability

The Heat Tranfer in the simulation process maximum through conduction, with less contribution by convection and radiation. The inclusion of temperature-dependent material properties significantly improves the accuracy of the thermal prediction.

Radiation and convection effects become more significant at higher temperatures, particularly near the weld pool region. The moving heat source model successfully captures the transient heat flow behavior and accurately reproduces the temperature evolution during welding.

Since the numerical predictions closely match experimental observations, the developed model can be considered reliable for further structural analysis. The transient temperature field can be directly used as thermal loading input for residual stress and distortion analysis in future studies.

4.7 Overall Discussion

Overall, the transient thermal analysis demonstrates that SS304L exhibits highly localized heating with steep thermal gradients during welding. The thermal cycles obtained from simulation clearly explain the formation of the weld zone and heat-affected zone. It is evident from the results that the predicted temperature distribution through the above mentioned ANSYS Parametric Design Language is closely matching with the values derived through experimental temperature distribution. Also the heat source movement has been made based on the actual weld speed and the weld heat movement was clearly shown. The temperature dissipation shows that the radiation mode of heat transfer super imposed over the convective heat transfer co-efficient effectively transfers the heat. All the material properties involved in transient thermal analysis were specified with variation in temperature. As a close to accurate temperature profile has been generated, the same can be used as input of thermal load to the next phase of analysis. A strong agreement between numerical predictions and experimental observations demonstrates the accuracy and reliability of the ANSYS APDL-based model in capturing welding thermal behaviour. Moreover, the validated simulation approach can be extended to more complex geometries, such as butt welding of tubes in heat

International Journal of Engineering Research & Technology (IJERT)
ISSN: 2278-0181
Vol. 15 Issue 06 , June - 2026

exchanger systems and to evaluate the deformation as well as shrinkages in cladding process on shells, to effectively study temperature evolution and process performance.

5.0 CONCLUSIONS

The procedure for transient thermal analysis is developed using the commercial software ANSYS effectively accounts temperature dependant material properties, solidification of weld metal as well as convective and radiative modes of heat transfer boundary conditions. The various welding passes in the weld joints are simulated using ANSYS birth and death features. The theoretically estimated results are validated against the experimental values, which are found matching excellently. The validated procedure is used for the estimation of temperature distribution in weld joints of advanced heat exchanger tubes.

6.0 REFERENCES

[1] 1. Murugan.S, Sanjai K Rai, P.V.Kumar, T.Jayakumar, Baldev Raj, M.S.C.Bose (2001), “Temperature distribution and residual stresses due to mult ipass welding in type 304 stainless steel and low carbon steel weld pads”, International Journal of Pressure Vessel and Piping,Vol.78,pp.307-317

[2] 2. Xiangyang Lu and Tasnim Hassan (2001), “Residual stresses in butt and socket welded joints”, Transactions, SMiRT 16

[3] 3. Murugan.S, P.V.Kumar, T.P.S.Gill, B.Raj, M.S.C.Bose (1999), “Numerical modelling and experimental determination of temperature distribution during manual metal arc welding”, Science and Technology of Welding and Joining, Vol.4

[4] 4. Barsoum, “Residual stress prediction and relaxation in welded tubular joint”

[5] 5. Dragi Stamenkovic, Ivana Vasovic, “Finite Element Analysis of Residual stress in butt welding two similar plates”, Scientific Technical Review,Vol.1,2009

[6] 6. Fanrang Kong, Radovan Kovacevic,“3D Finite element modelling of the thermally induced residual stress in the hybrid laser/arc welding of lap joint”, Journal of Material Processing Technology210(2010),pp.941-950

[7] 7. Andrea Capriccio, Paolo Froze, “Multipurpose ANSYS FE procedure for welding process simulation”, Fusion Engineering and Design (2009)

[8] 8. G.Labeas, S.Tsirkas, J.Diamantakos and A.Kermanidis, “Effect of residual stresses due to laser welding on the stress intensity factors of adjacent crack”, ISTRAM

[9] 9. E.Pardo and D.C.Weckman, “Prediction of weld pool and reinforcement dimensions of GMA welds using a finite element model”, Metall. Trans. B, 1989, 20B, 937-947

[10] 10. T.Zacharia, S.A.David and J.MVitek, “Effect of evaporation and temperature dependent material properties on weld pool development”, Metall. Trans. B, 1991, 22B, 233-241

[11] 11. K.Easterling, “Introduction to the physical metallurgy of welding”, 2nd edn; 1992, Oxford, Butterworth Heinemann